

Electronic Supplementary Information

Electrocatalytic oxygen reduction with cobalt corroles bearing cationic substituents

Yimei Gao, Haitao Lei,* Zijia Bao, Xinrong Liu, Lingshuang Qin, Zhiyuan Yin,
Huiyuan Li, Shu Huang, Wei Zhang, and Rui Cao*

*Key Laboratory of Applied Surface and Colloid Chemistry, Ministry of Education,
School of Chemistry and Chemical Engineering, Shaanxi Normal University, Xi'an
710119, China.*

*Correspondence E-mail: leiht2017@snnu.edu.cn; ruicao@snnu.edu.cn

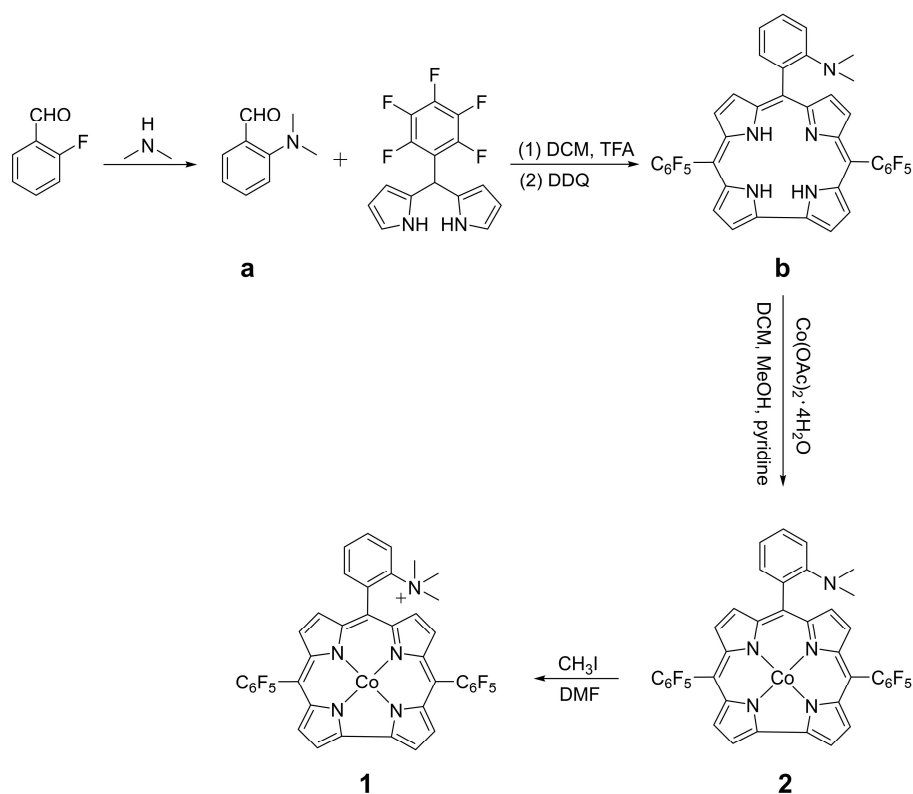
General Methods and Materials.

Manipulations of air- and moisture-sensitive materials were performed under an atmosphere of argon gas using the standard Schlenk line technique. All reagents were purchased from commercial suppliers and were used as received unless otherwise noted. Dry solvents, including acetonitrile, dichloromethane, and chloroform were dried by distillation with CaH₂. Tetrabutylammonium hexafluorophosphate (*n*-Bu₄NPF₆) was recrystallized from absolute alcohol. All aqueous solutions were prepared freshly using Milli-Q water. Carbon nanotubes (CNTs, >95% purity, <8 nm outside diameter, 3 nm inside diameter) were purchased from Chengdu Organic Chemicals Co. Ltd.

High-resolution mass spectra (HRMS) were acquired using a Brüker MAXIS. ¹H NMR spectra were acquired on a JEOL spectrometer operating at 400 MHz. Electronic absorption spectra were measured using a Hitachi U-3310 spectrophotometer. Hitachi SU8020 cold-emission field emission scanning electron microscope (FE-SEM) was used to study the sample morphology with an accelerating voltage of 1 kV. Transmission electron microscopy (TEM) images were obtained using JEOL JEM-2100 with a 200 kV accelerating voltage. X-ray photoelectron spectroscopy (XPS) data were collected by ESCALab 250-XI electron spectrometer from Thermo Fisher Scientific.

Synthesis of Co Corroles.

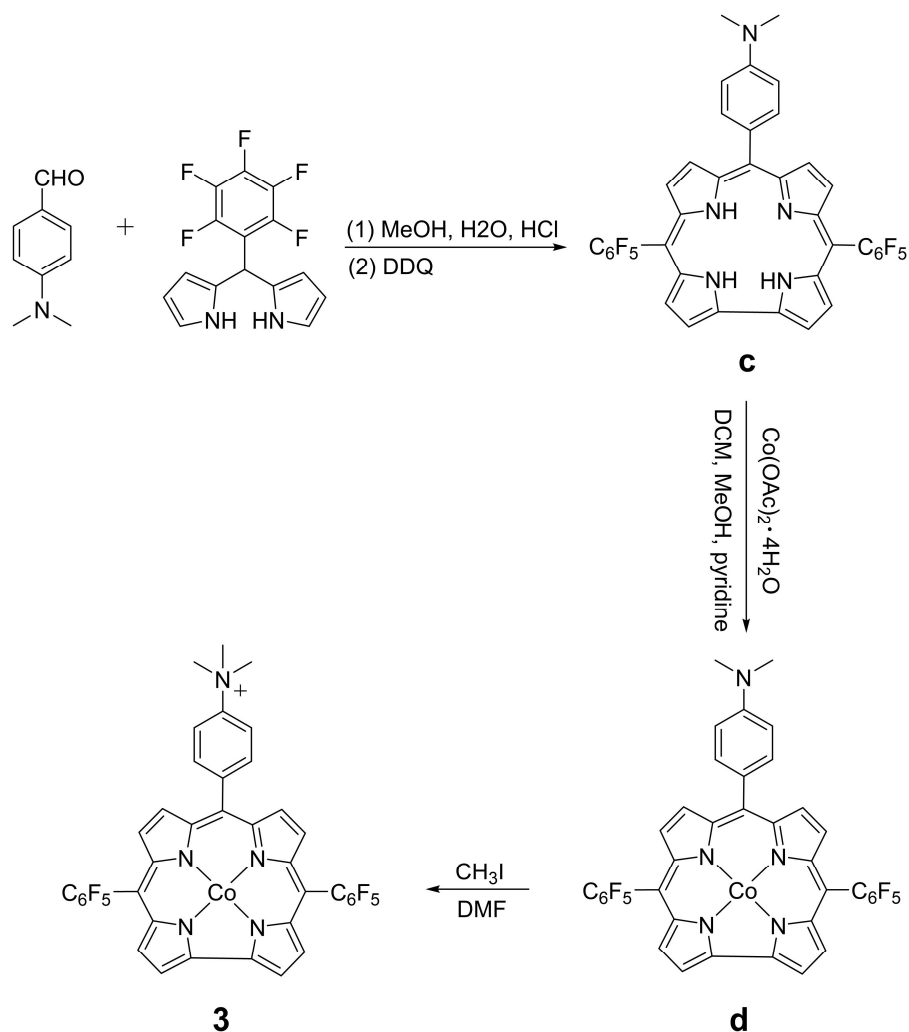
The synthetic route of Co corroles is depicted in Scheme S1 and S2.



Scheme S1. Synthetic route of Co corroles **1** and **2**.

Synthesis of a. To an anhydrous DMF (10 mL) under N₂, were slowly added 2-fluorobenzaldehyde (548 μL, 5.21 mmol), dimethylamine (335 μL, 6.70 mmol) and potassium carbonate (7.2 g, 52 mmol). The resulted suspension was refluxed at 110 °C for 36 h. Subsequently, the reaction mixture was poured into water and extracted with dichloromethane. The combined organic layers were dried with Na₂SO₄, filtered, and the solvent was removed by a rotary evaporator. The crude product was purified by silica-gel column chromatography (hexane/DCM = 10:1 v/v) to afford a pale-yellow oil. Recrystallization from hexane gave yellow crystals of **a** (525 mg, yield 68%). ¹H NMR (400 MHz, CDCl₃): δ = 10.23 (s, 1H), 7.72 (t, *J* = 4.8 Hz, 1H), 7.47 (dd, *J* = 4.8 Hz, 1H), 7.03 (m, 2H), 2.87 (s, 6H) ppm.

Synthesis of b. To 50 mL of dichloromethane, were added **a** (238 mg, 1.6 mmol) and 5-(pentafluorophenyl)dipyrromethane (1 g, 3.2 mmol). To the resulted solution, trifluoroacetic acid (48 μ L) was added with stirring. After the mixture was stirred for 3 h at room temperature under dark, a solution of chloranil (472 mg, 1.92 mmol) in toluene-tetrahydrofuran (2 mL) was added, and the resulted solution was stirred at room temperature for a further 30 min. The resulted solution was poured into water and extracted with dichloromethane. The combined organic layers were dried with Na₂SO₄, filtered, and the solvent was removed by a rotary evaporator. The crude product was purified by silica-gel column chromatography (hexane/DCM = 8:1 v/v) to afford solids of complex **b** (60 mg, yield 5%). ¹H NMR (400 MHz, CDCl₃): δ = 9.07 (d, J = 4.3 Hz, 2H), 8.70-8.64 (m, 4H), 8.53 (d, J = 4.3 Hz, 2H), 7.84 (d, J = 7.4 Hz, 1H), 7.69 (t, J = 8.8 Hz, 1H), 7.44 (d, J = 8.3 Hz, 1H), 7.33 (t, J = 8.8 Hz, 1H), 2.28 (s, 6H) ppm. HRMS: Calcd for C₃₉H₂₂F₁₀N₅ [M+H]⁺, 750.1710; found, 750.1718 (Fig. S1). Anal. calcd for C₃₉H₂₁F₁₀N₅: C, 62.49; H, 2.82; N, 9.34. Found: C, 62.61; H, 2.93; N, 9.41.



Scheme S2. Synthetic route of Co corrole **3**.

Synthesis of c. Sample of 4-dimethylaminobenzaldehyde (238 mg, 1.6 mmol) and 5-(pentafluorophenyl)dipyrromethane (1 g, 3.2 mmol) were added to 160 mL methanol, followed by the addition of a HCl solution (36%, 7.7 mL) in H₂O (160 mL). After stirring for 3 h at room temperature under dark, the mixture was washed with water, extracted with chloroform, and dried with Na₂SO₄. After concentrating the solution to about 100 mL on a rotary evaporator, a solution of chloranil (785 mg, 3.2 mmol) in toluene-tetrahydrofuran (2 mL) was added, and the reaction was stirred at room temperature for a further 30 min. The organic solvent was then removed by a rotary evaporator to give the crude product, which was purified by silica-gel column

chromatography (hexane/DCM = 5:1 v/v) to afford solids of complex **c** (132 mg, yield 11 %). ^1H NMR (400 MHz, CDCl_3): δ = 9.10 (d, J = 4.3 Hz, 2H), 8.80 (d, J = 4.7 Hz, 2H), 8.69 (d, J = 4.7 Hz, 2H), 8.56 (d, J = 4.3 Hz, 2H), 8.10 (d, J = 8.5 Hz, 2H), 7.10 (d, J = 8.5 Hz, 2H), 3.20 (s, 6H) ppm. HRMS: Calcd for $\text{C}_{39}\text{H}_{22}\text{F}_{10}\text{N}_5$ $[\text{M}+\text{H}]^+$, 750.1710; found, 750.1715 (Fig. S2). Anal. calcd for $\text{C}_{39}\text{H}_{21}\text{F}_{10}\text{N}_5$: C, 62.49; H, 2.82; N, 9.34. Found: C, 62.69; H, 2.91; N, 9.43.

Synthesis of d. Complex **c** (50 mg, 0.067 mmol), $\text{Co}(\text{OAc})_2 \cdot 4\text{H}_2\text{O}$ (167 mg, 0.67 mmol) and pyridine (50 μL) were dissolved in dichloromethane and methanol (15 mL). After stirring for 1 h at room temperature, the reaction mixture was poured into water and extracted with dichloromethane. The combined organic layers were dried with Na_2SO_4 , filtered, and the solvent was removed by a rotary evaporator. The crude product was purified by silica-gel column chromatography (hexane/DCM/pyridine = 2:1:0.01 v/v) to afford solids of complex **d** (48 mg, yield 74%). ^1H NMR (400 MHz, CDCl_3): δ = 9.13 (d, J = 4.3 Hz, 2H), 8.87-8.78 (m, 4H), 8.62 (d, J = 4.3 Hz, 2H), 7.92 (d, J = 8.2 Hz, 2H), 7.03 (d, J = 8.3 Hz, 2H), 5.94 (brs, 2H), 5.04 (brs, 4H), 3.18 (s, 6H), 0.88 (brs, 4H) ppm. HRMS: Calcd for $\text{C}_{39}\text{H}_{18}\text{CoF}_{10}\text{N}_5$ $[\text{M} - 2\text{py}]^+$, 805.0729; found, 805.0715 (Fig. S3). Anal. calcd for $\text{C}_{49}\text{H}_{28}\text{CoF}_{10}\text{N}_7$: C, 61.07; H, 2.93; N, 10.17. Found: C, 61.26; H, 3.17; N, 10.33.

Preparation of Catalyst-Loaded Electrodes.

In a typical procedure, to 0.96 mL (acetonitrile/isopropyl alcohol = 2:1, v/v) solution containing 1.0 mg carbon nanotubes (CNT) and 1.0 mg Co corroles, was added 40 μL 5% Nafion (5 wt %, Dupont). The mixture was sonicated in an ultrasonic cleaner for 30 min. The suspension was applied to the surface of RDE or RRDE disk (10 μL)

and GC (4 μL) electrodes using a pipet. The electrodes were then dried slowly under dark for later electrocatalytic studies.

Electrochemical Studies.

Electrochemical measurements were performed using CH Instruments (CHI 660D Electrochemical Analyzer) at 25 °C. Cyclic voltammograms (CVs) were collected in dry acetonitrile (5 mL) containing 0.5 mM Co corroles and 0.1 M *n*-Bu₄NPF₆ using a three-compartment cell with a 0.07 cm² glassy carbon (GC) working electrode, graphite rod counter electrode, and Ag/AgNO₃ reference electrode (BASi, 10 mM AgNO₃, 0.1 M *n*-Bu₄NPF₆ in acetonitrile). The solution was bubbled with high-purity argon for at least 30 min before analysis. Ferrocene was added at the end of the measurement as an internal standard. Electrocatalytic ORR measurements were made in 0.5 M H₂SO₄ and neutral 0.1 M phosphate buffer solutions by using Biopotentiostat (model DY2300 Electrochemical Analyzer) in a conventional three-electrode system with rotating-ring disk electrode (RRDE) and rotating disk electrode (RDE) loaded with catalysts as the working electrode, carbon rod as the counter electrode, and Ag/AgCl (saturated KCl solution) as the reference electrode. The geometric parameters of RRDE are: platinum ring electrode (0.188 cm²) and GC disk electrode (0.125 cm²). The collection coefficient of 0.42 was evaluated for this RRDE using the [Fe(CN)₆]^{3-/4-} redox couple. Linear sweep voltammograms (LSVs) were measured in O₂-saturated 0.5 M H₂SO₄ and neutral 0.1 M phosphate buffer solutions at 5 mV s⁻¹ scan rate. The ring electrode was polarized at 1.26 V in 0.5 M H₂SO₄ solutions and 0.80 V in neutral 0.1 M phosphate buffer solutions. Tafel plots were calculated by measuring LSV data at 2 mV s⁻¹ scan rate and 1600 rpm rotation speed. The number (*n*) of electrons transferred during ORR was determined:

From RRDE analysis:

$$n = 4 \times \frac{I_d}{I_d + \frac{I_r}{N}}$$

From Koutecky-Levich (K-L) analysis:

$$\frac{1}{j} = \frac{1}{j_k} + \frac{1}{j_d} = \frac{1}{nFkC_{O_2}} + \frac{1}{0.2nFD_{O_2}^{2/3}\nu^{-1/6}C_{O_2}\omega^{1/2}}$$

in which I_d is the disk current, I_r is the ring current, and $N = 0.42$ (RRDE) is the current collection efficiency of the Pt ring electrode; j is the current density, j_k and j_d are the kinetic and diffusion-limited current densities, respectively, ω is the electrode rotation rate, n is the transferred electron number per O_2 , F is the Faraday constant (96485 C mol^{-1}), C_{O_2} is the bulk concentration of O_2 ($1.13 \times 10^{-6} \text{ mol cm}^{-3}$ in $0.5 \text{ M H}_2\text{SO}_4$, $1.20 \times 10^{-6} \text{ mol cm}^{-3}$ in neutral 0.1 M phosphate buffer solutions), D_{O_2} is the diffusion coefficient of O_2 ($1.50 \times 10^{-5} \text{ cm}^2 \text{ s}^{-1}$ in $0.5 \text{ M H}_2\text{SO}_4$, $1.96 \times 10^{-5} \text{ cm}^2 \text{ s}^{-1}$ in neutral 0.1 M phosphate buffer solutions), ν is the kinematic viscosity of the electrolyte ($0.01 \text{ cm}^2 \text{ s}^{-1}$). The constant 0.2 is adopted when the rotation speed is expressed in rpm.

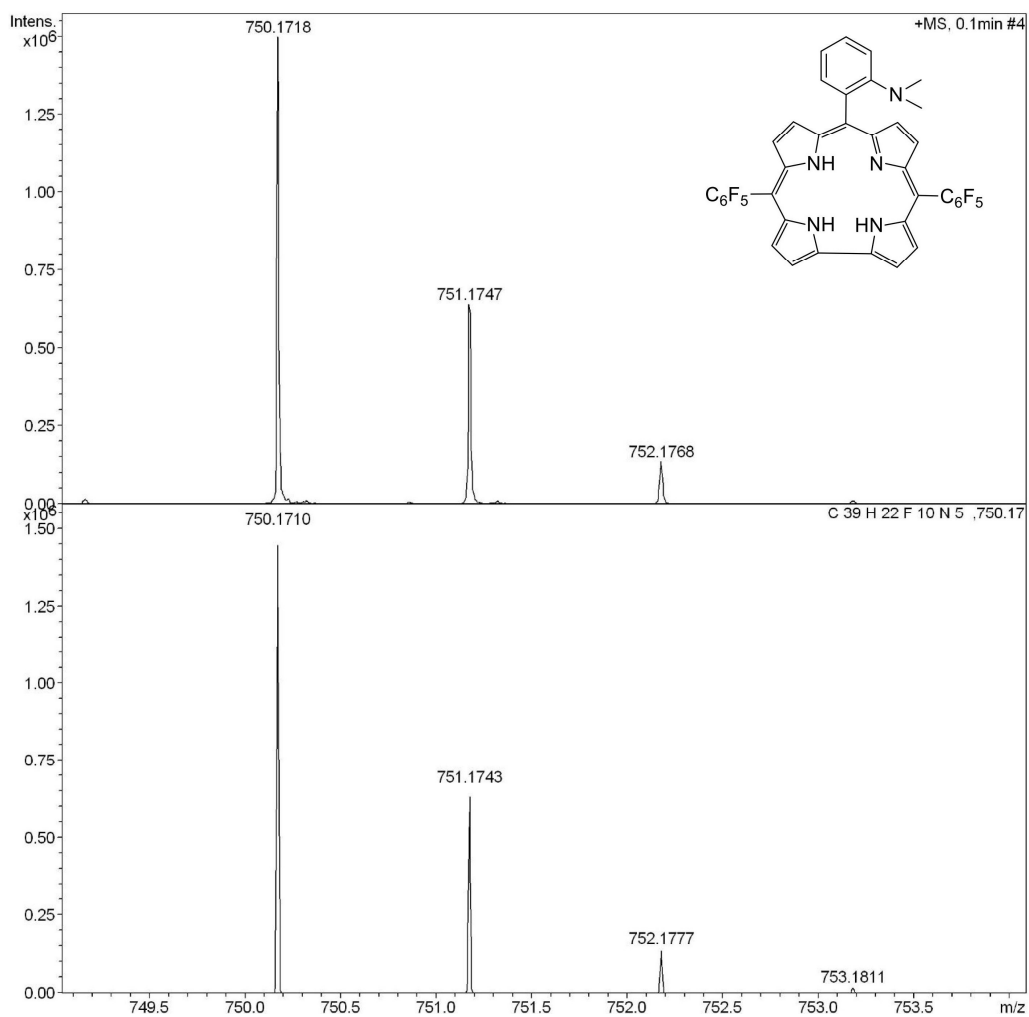


Fig. S1. HRMS of **b** in methanol, showing the ion at a mass-to-charge ratio of 750.1718. This value is consistent with the calculated number of 750.1710 for the monocation of $[M + H]^+$ ($M = C_{39}H_{21}F_{10}N_5$).

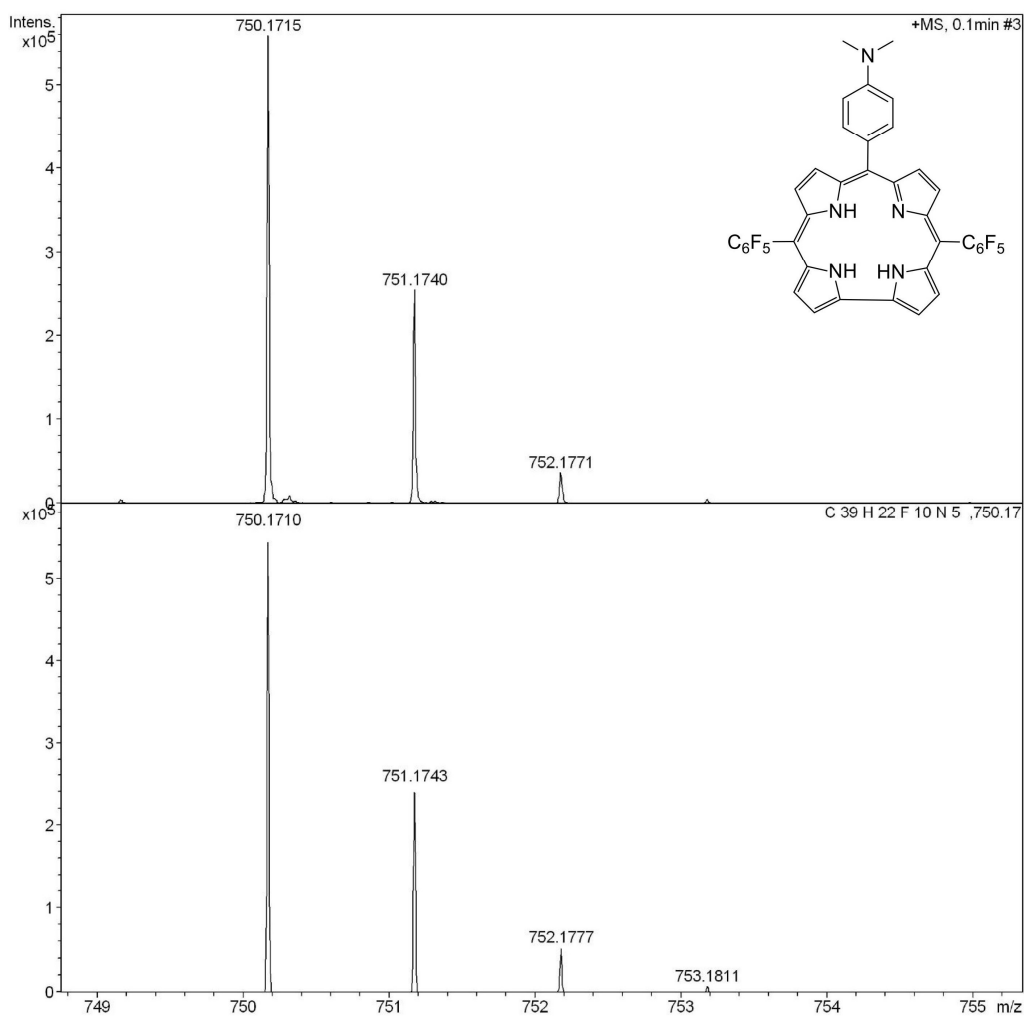


Fig. S2. HRMS of **c** in methanol, showing the ion at a mass-to-charge ratio of 750.1715. This value is consistent with the calculated number of 750.1710 for the monocation of $[M + H]^+$ ($M = C_{39}H_{21}F_{10}N_5$).

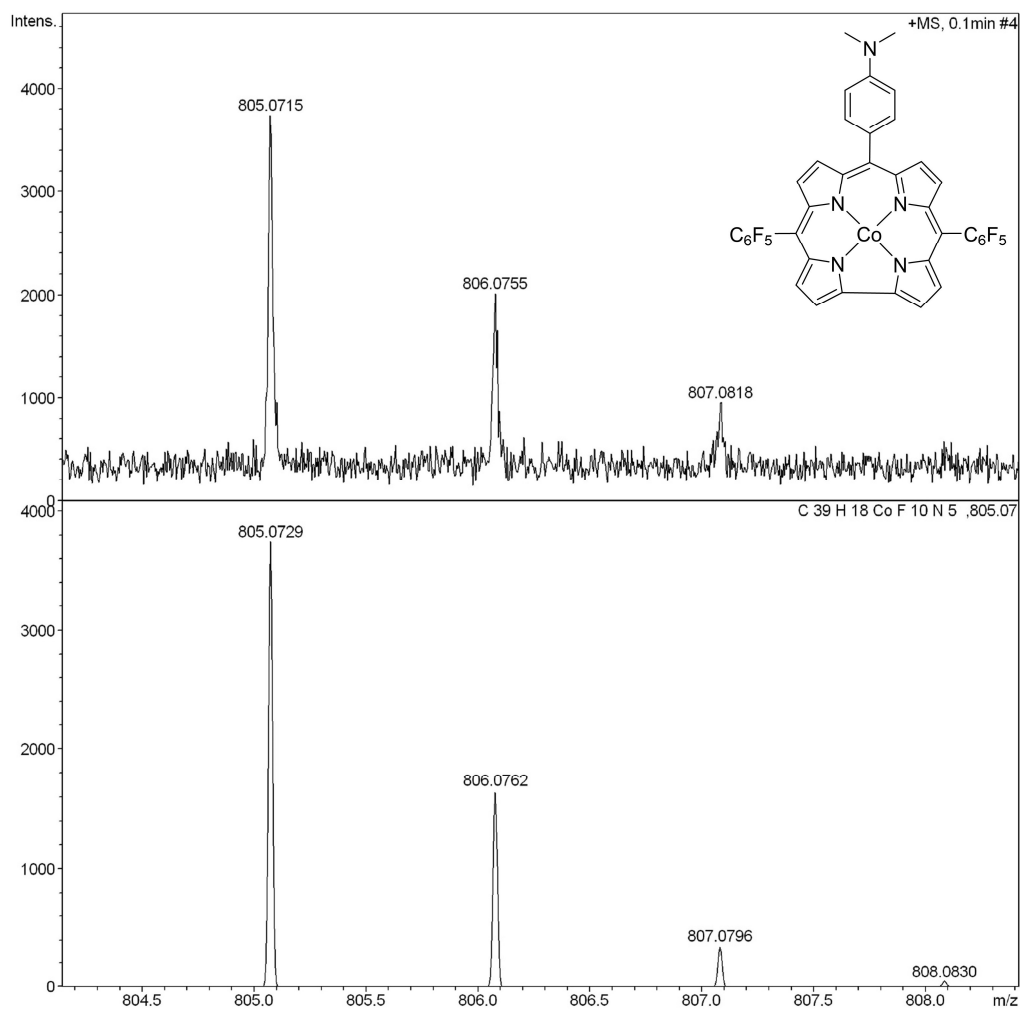


Fig. S3. HRMS of **d** in methanol, showing the ion at a mass-to-charge ratio of 805.0715. This value is consistent with the calculated number of 805.0729 for the monocation of $[C_{39}H_{18}CoF_{10}N_5]^+$. Note that the two axial pyridines were dissociated during mass spectrometry measurements.

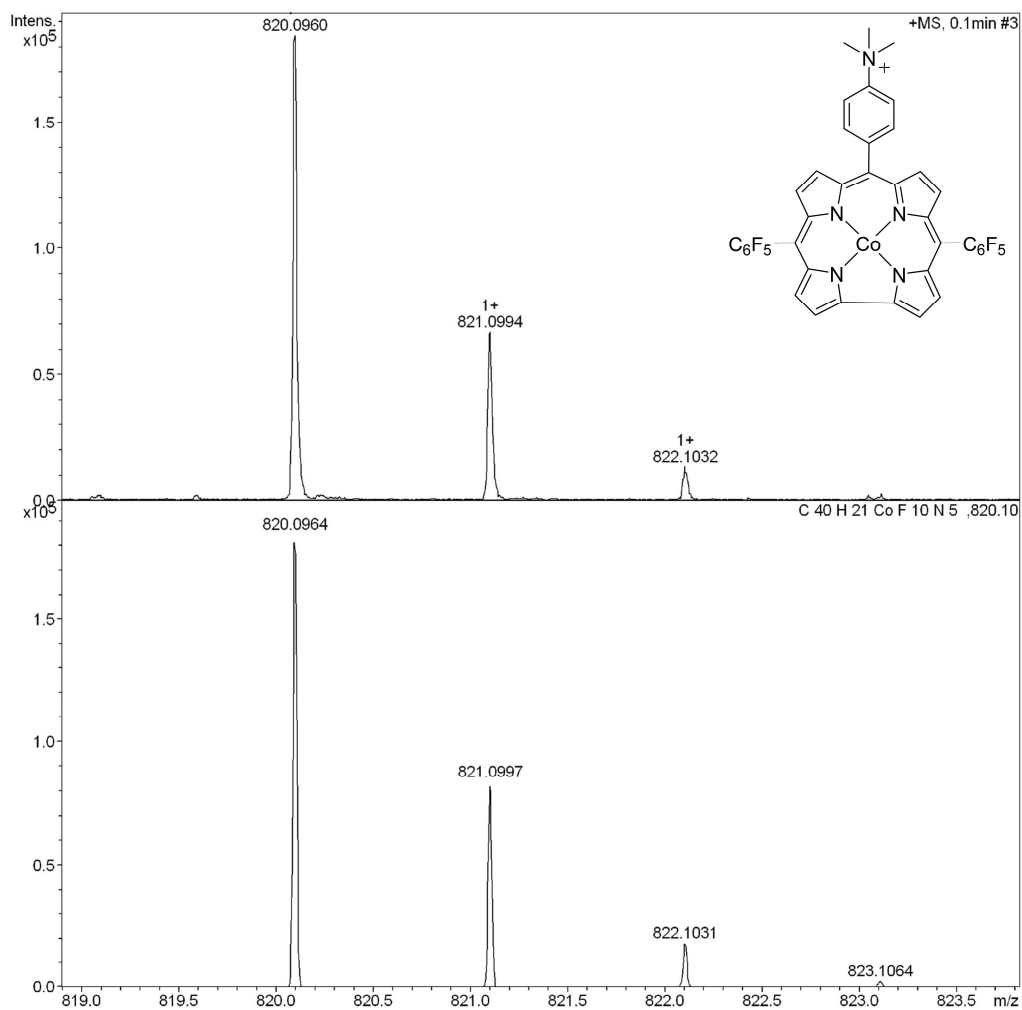


Fig. S4. HRMS of **3** in methanol, showing the ion at a mass-to-charge ratio of 820.0960. This value is consistent with the calculated number of 820.0964 for the monocation of $[C_{40}H_{21}CoF_{10}N_5]^+$.

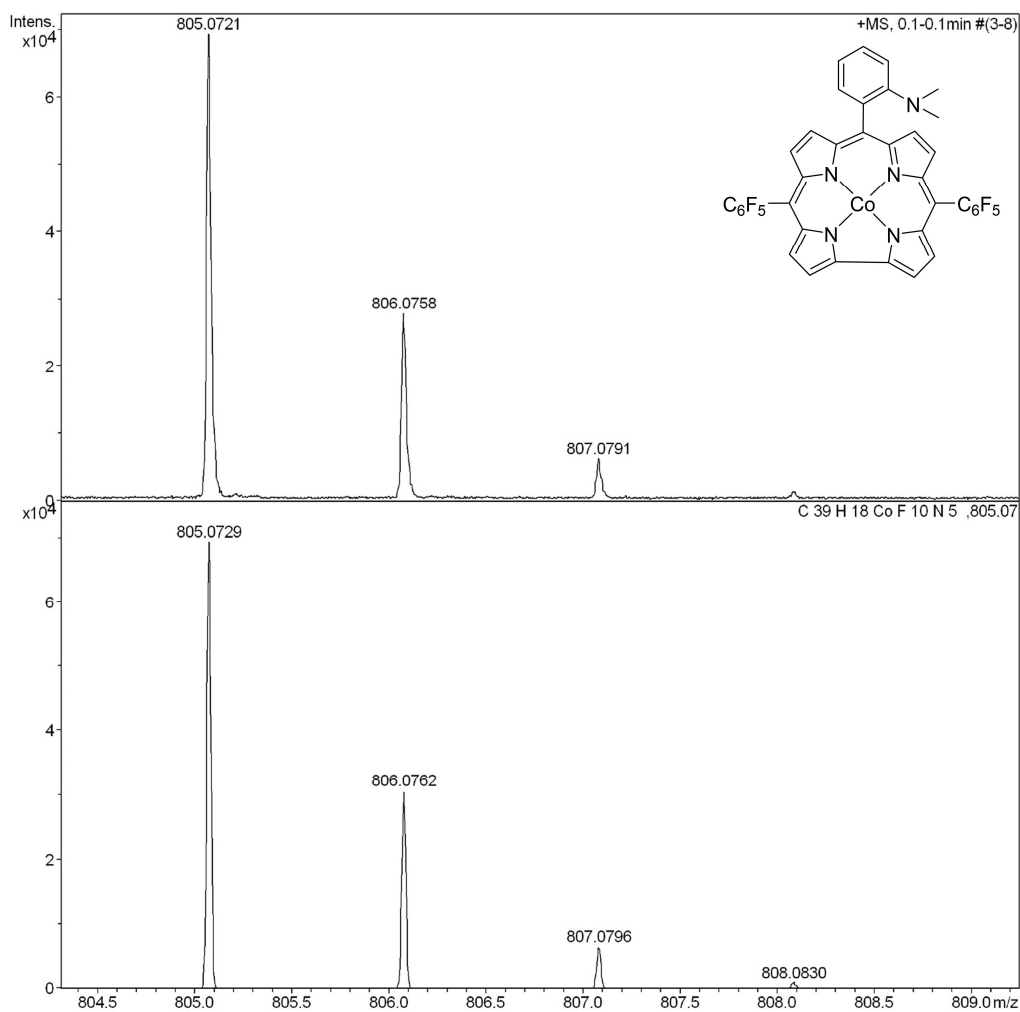


Fig. S5. HRMS of **2** in methanol, showing the ion at a mass-to-charge ratio of 805.0721. This value is consistent with the calculated number of 805.0729 for the monocation of $[C_{39}H_{18}CoF_{10}N_5]^+$. Note that the two axial pyridines were dissociated during mass spectrometry measurements.

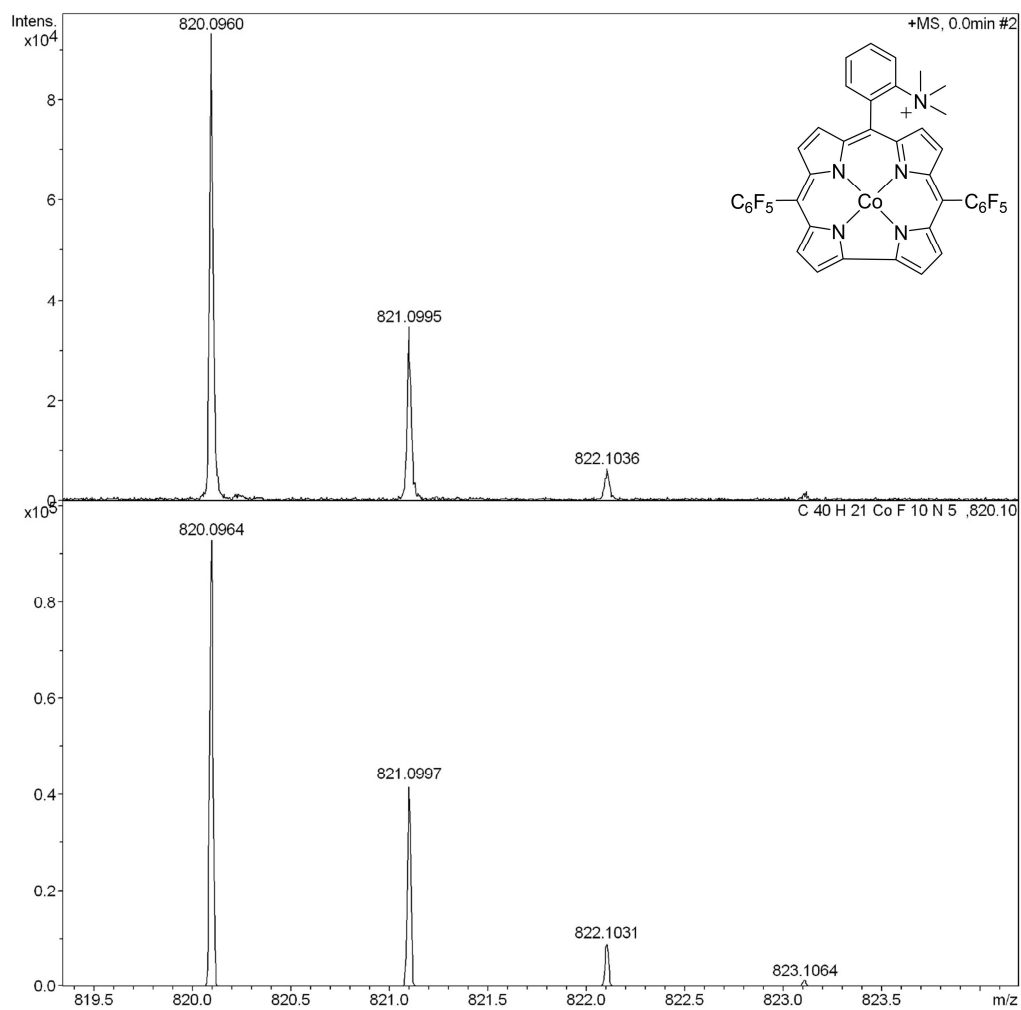


Fig. S6. HRMS of **1** in methanol, showing the ion at a mass-to-charge ratio of 820.0960. This value is consistent with the calculated number of 820.0964 for the monocation of [C₄₀H₂₁CoF₁₀N₅]⁺.

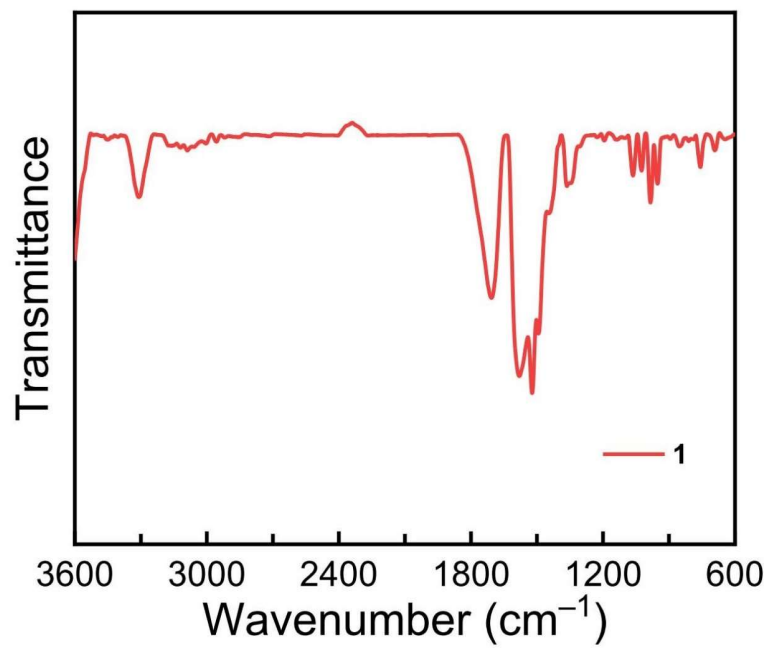


Fig. S7. FTIR transmission spectrum of **1** in a KBr pellet.

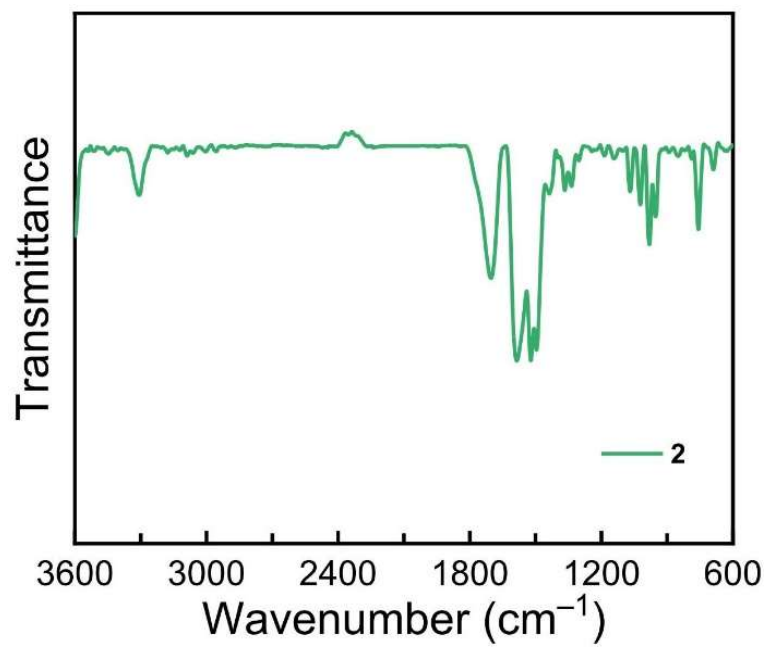


Fig. S8. FTIR transmission spectrum of **2** in a KBr pellet.

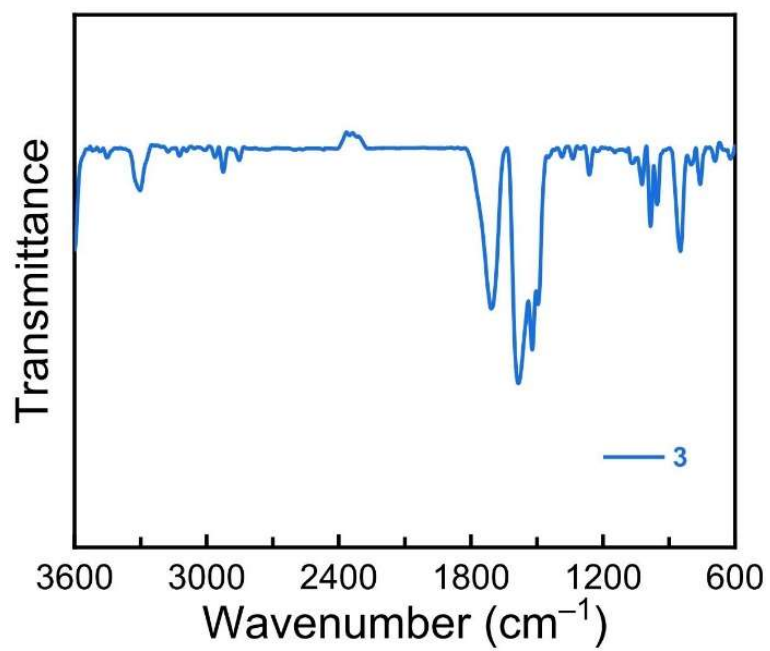


Fig. S9. FTIR transmission spectrum of **3** in a KBr pellet.

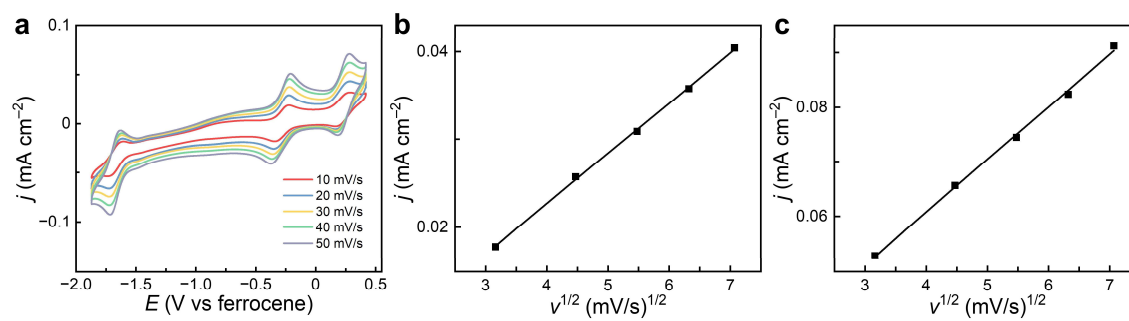


Fig. S10. (a) CVs of 0.5 mM **1** under argon with different scan rates in acetonitrile. Plots of the Co^{III/II} (b) and Co^{II/I} (c) reduction peak currents of **1** on the square root of scan rates. Conditions: 0.1 M *n*-Bu₄NPF₆, GC working electrode, 25 °C.

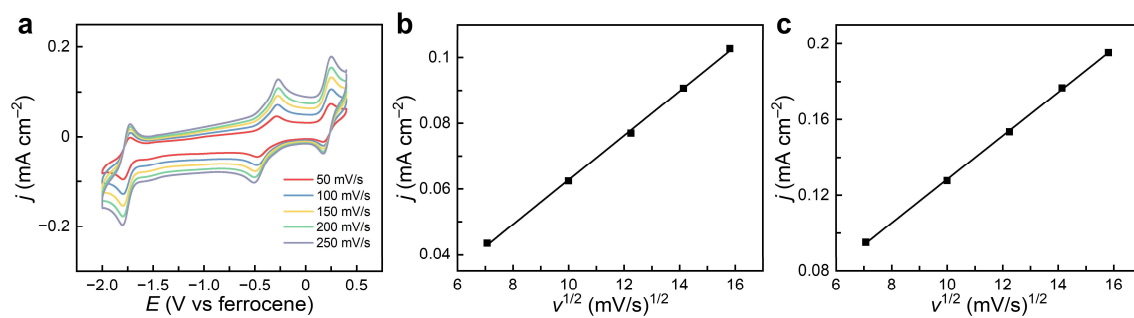


Fig. S11. (a) CVs of 0.5 mM **2** under argon with different scan rates in acetonitrile. Plots of the Co^{III/II} (b) and Co^{II/I} (c) reduction peak currents of **2** on the square root of scan rates. Conditions: 0.1 M *n*-Bu₄NPF₆, GC working electrode, 25 °C.

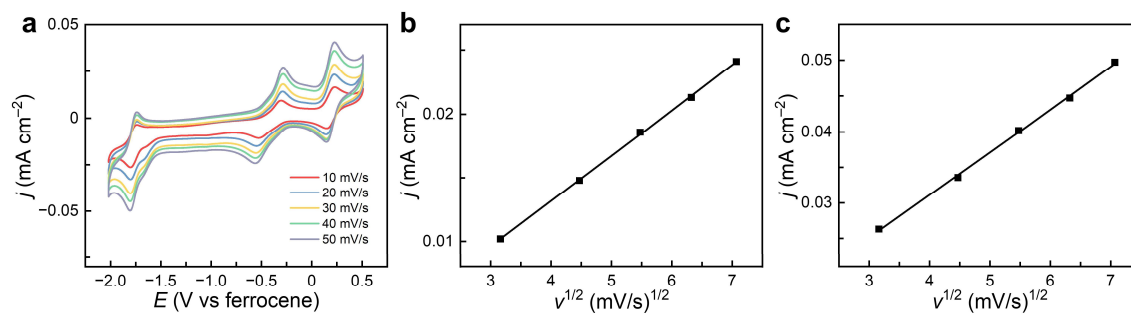


Fig. S12. (a) CVs of 0.5 mM **3** under argon with different scan rates in acetonitrile. Plots of the Co^{III/II} (b) and Co^{II/I} (c) reduction peak currents of **3** on the square root of scan rates. Conditions: 0.1 M *n*-Bu₄NPF₆, GC working electrode, 25 °C.

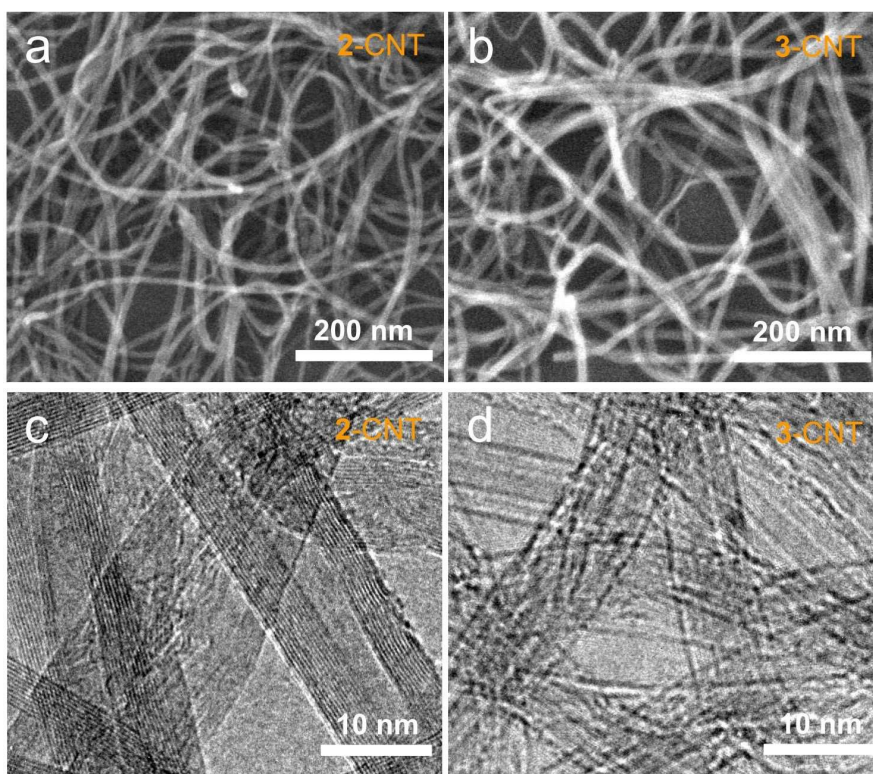


Fig. S13. SEM images of **2-CNT** (a) and **3-CNT** (b). TEM images of **2-CNT** (c) and **3-CNT** (d).

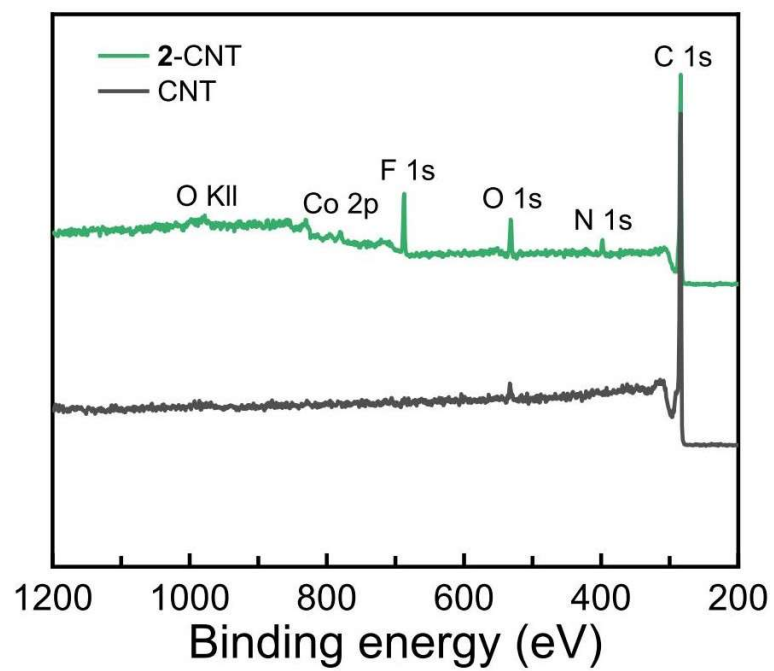


Fig. S14. Full XPS spectra of 2-CNT and blank CNT.

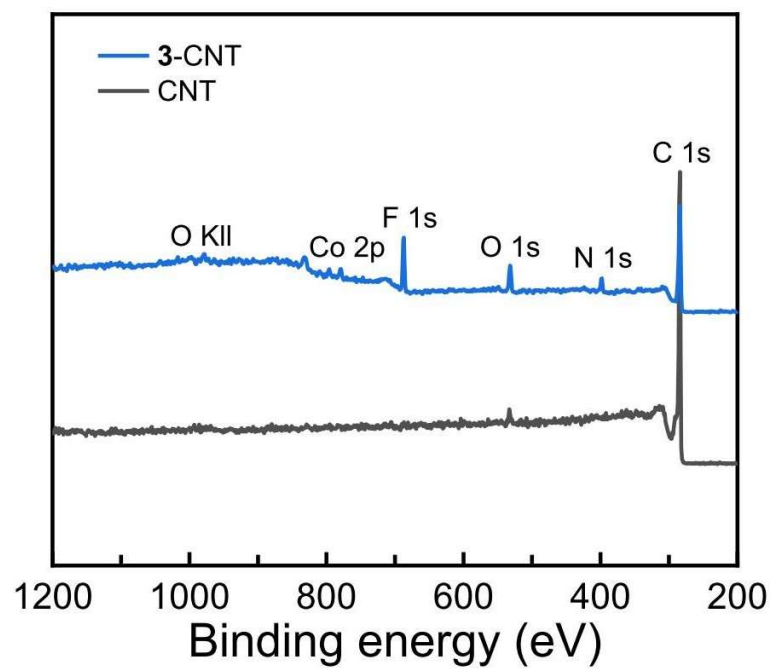


Fig. S15. Full XPS spectra of 3-CNT and blank CNT.

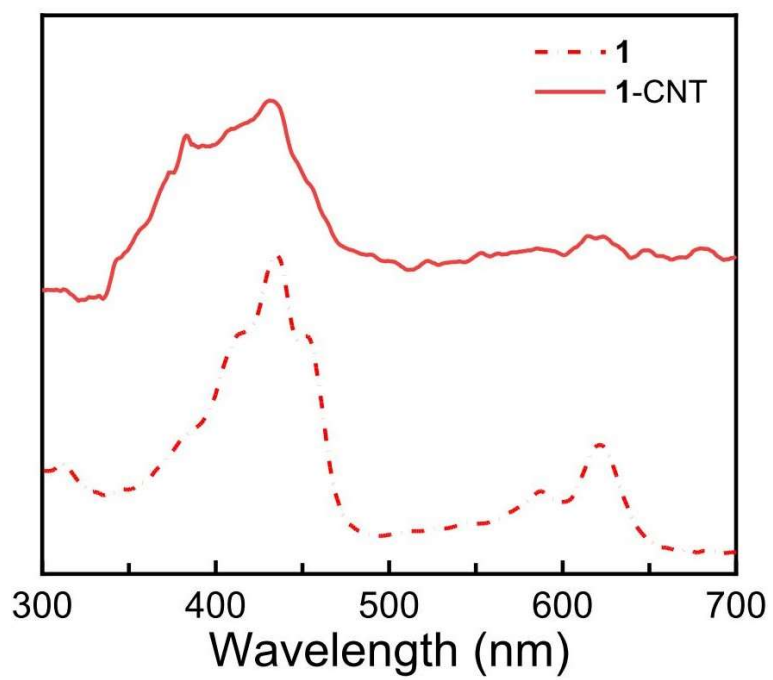


Fig. S16. UV-vis spectra of **1** and **1-CNT** in acetonitrile.

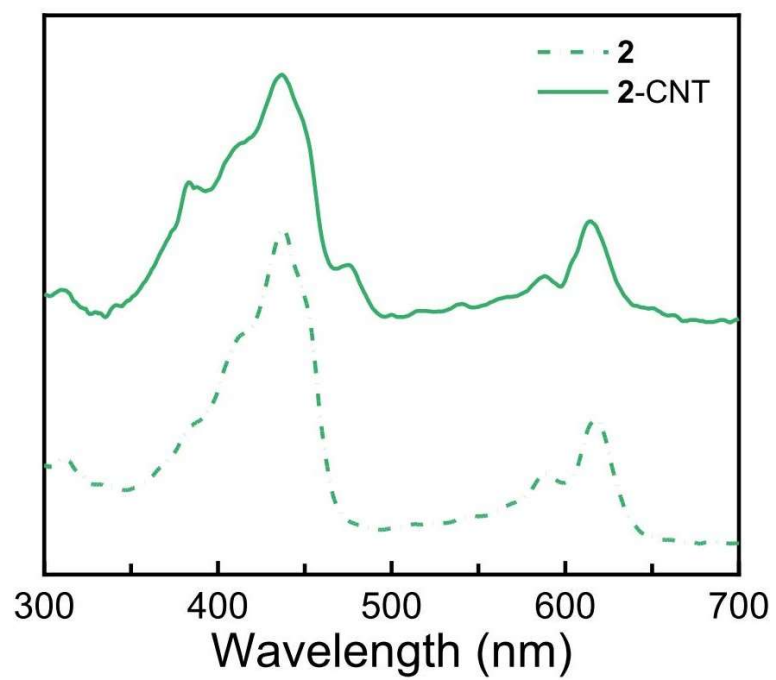


Fig. S17. UV-vis spectra of **2** and **2-CNT** in acetonitrile.

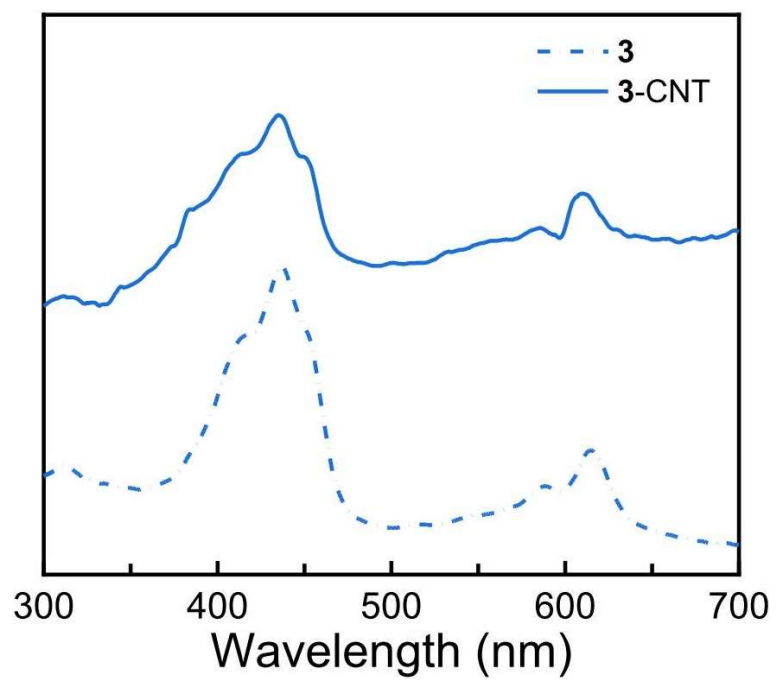


Fig. S18. UV-vis spectra of **3** and **3-CNT** in acetonitrile.

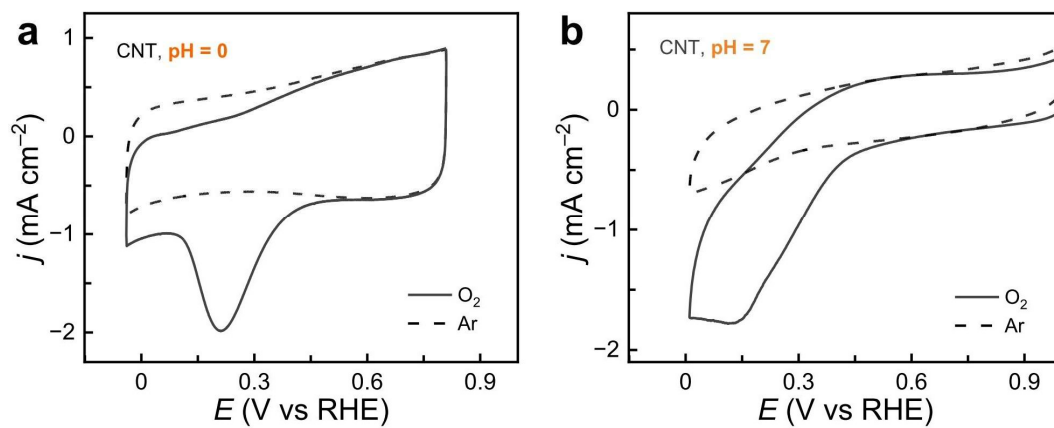


Fig. S19. (a) CVs of GC electrodes loaded with blank CNT under argon and O₂ in 0.5 M H₂SO₄ solutions. (b) CVs of GC electrodes loaded with blank CNT under argon and O₂ in neutral 0.1 M phosphate buffer solutions.

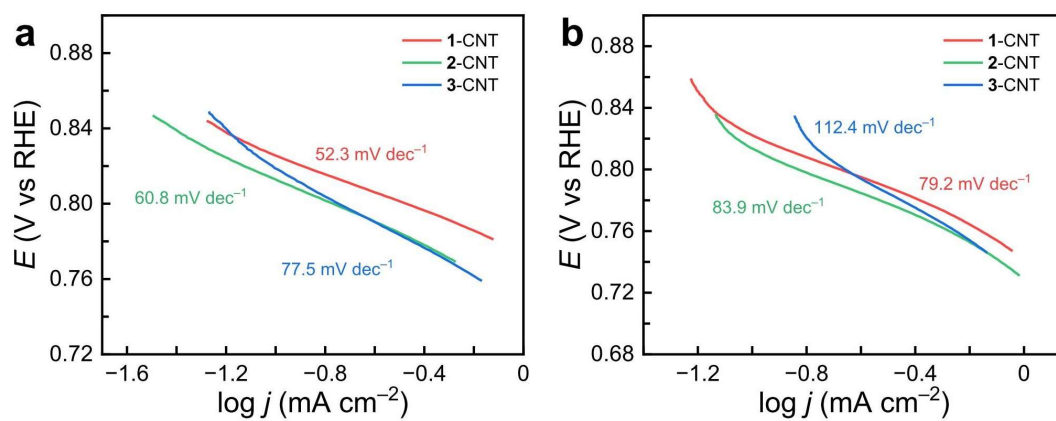


Fig. S20. (a) ORR Tafel slopes of **1-CNT**, **2-CNT** and **3-CNT** in O₂-saturated 0.5 M H₂SO₄ solutions. (b) ORR Tafel slopes of **1-CNT**, **2-CNT** and **3-CNT** in O₂-saturated neutral 0.1 M phosphate buffer solutions.

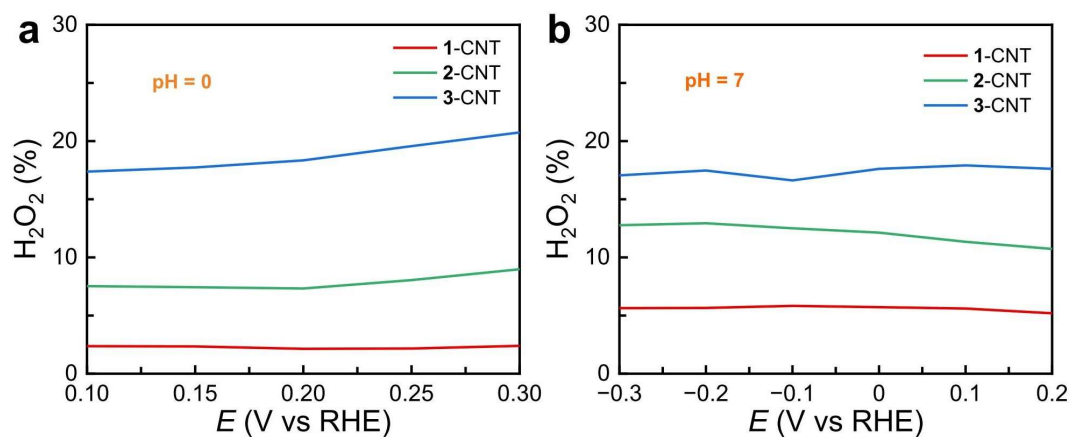


Fig. S21. (a) The H₂O₂ yield during electrocatalytic ORR with **1-CNT**, **2-CNT** and **3-CNT** measured in O₂-saturated 0.5 M H₂SO₄ solutions with RRDE electrode at 1600 rpm. (b) The H₂O₂ yield during electrocatalytic ORR with **1-CNT**, **2-CNT** and **3-CNT** measured in O₂-saturated neutral 0.1 M phosphate buffer solutions with RRDE electrode at 1600 rpm.

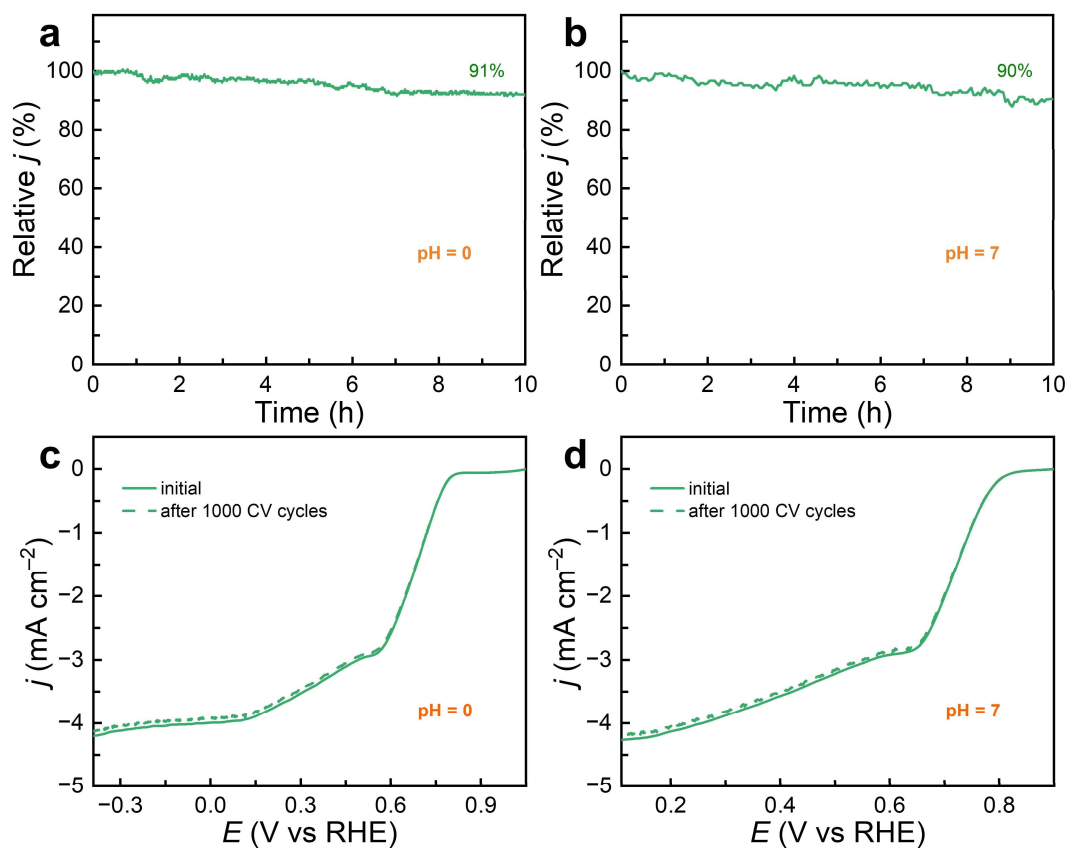


Fig. S22. Chronoamperometric measurements of GC electrode loaded with 2-CNT in a 0.5 M H_2SO_4 solution (a) and in a neutral 0.1 M phosphate buffer solution (b). LSVs using GC disk electrode loaded with 2-CNT before and after 1000 CV cycles in a 0.5 M H_2SO_4 solution (c) and in a neutral 0.1 M phosphate buffer solution (d). Conditions: GC disk electrode (area 0.125 cm^2), 1600 rpm rotation rate, 5 mV s^{-1} scan rate, $25 \text{ }^\circ\text{C}$.

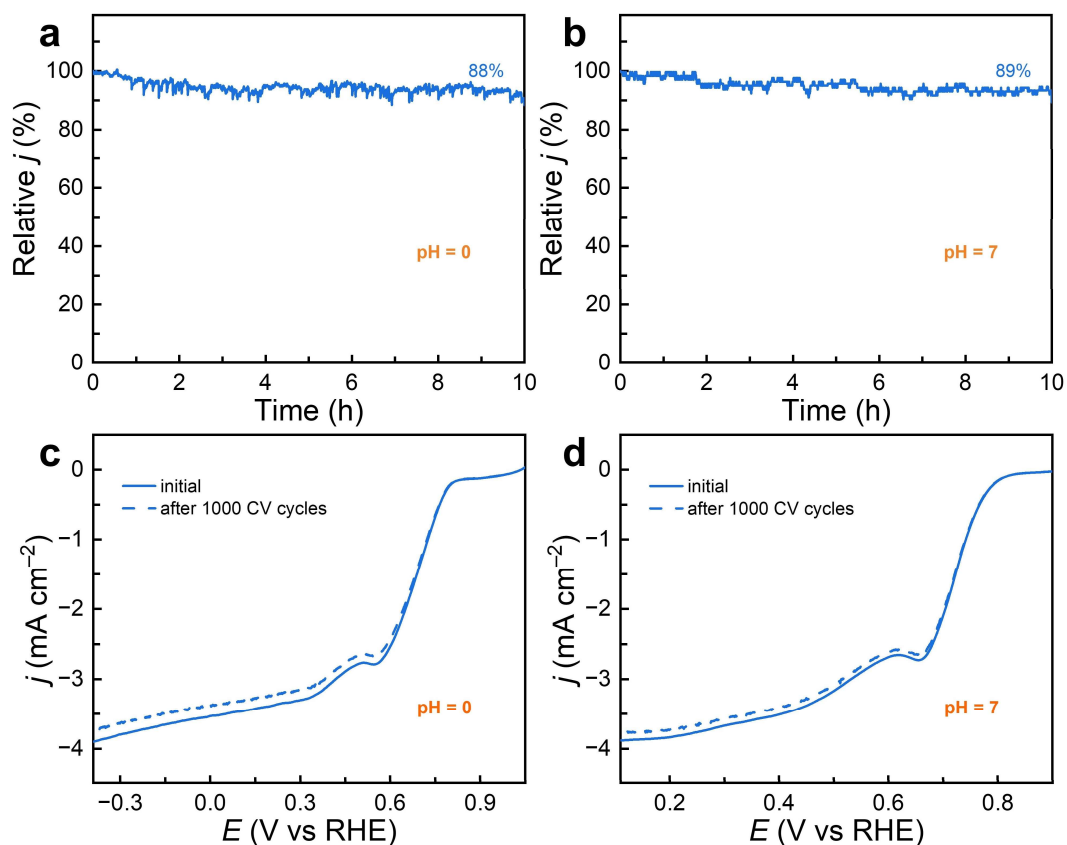


Fig. S23. Chronoamperometric measurements of GC electrode loaded with **3**-CNT in a 0.5 M H₂SO₄ solution (a) and in a neutral 0.1 M phosphate buffer solution (b). LSVs using GC disk electrode loaded with **3**-CNT before and after 1000 CV cycles in a 0.5 M H₂SO₄ solution (c) and in a neutral 0.1 M phosphate buffer solution (d). Conditions: GC disk electrode (area 0.125 cm²), 1600 rpm rotation rate, 5 mV s⁻¹ scan rate, 25 °C.

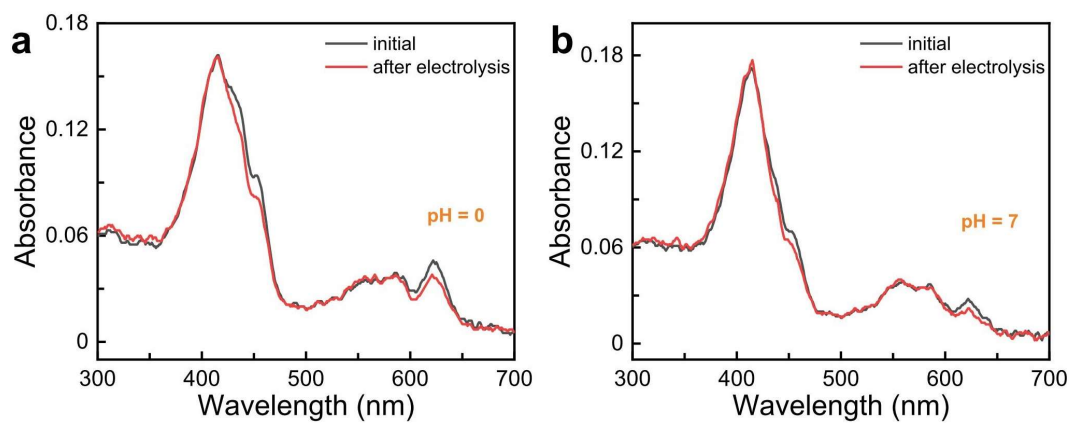


Fig. S24. (a) UV-vis spectra of **1** in acetonitrile before and after electrolysis in a 0.5 M H₂SO₄ solution. (b) UV-vis spectra of **1** in acetonitrile before and after electrolysis in a neutral 0.1 M phosphate buffer solution.

Table S1. Electrocatalytic ORR performance comparison for molecular electrocatalysts under acidic conditions.

Catalyst	Condition	$E_{1/2}$ (V vs RHE) ^a	n	Reference
1-CNT	0.5 M H ₂ SO ₄	0.75	3.93	This work
2-CNT	0.5 M H ₂ SO ₄	0.73	3.84	This work
3-CNT	0.5 M H ₂ SO ₄	0.72	3.63	This work
CNT-Cor-Co-C ₆ F ₅	0.5 M H ₂ SO ₄	0.61	3.61	<i>ACS Catal.</i> 2019 , 9, 4551-4560
CNT-Cor-Co-pyrene	0.5 M H ₂ SO ₄	0.61	3.61	<i>ACS Catal.</i> 2016 , 6, 6429-6437
CNT-Cor-Co-DPEN	0.5 M H ₂ SO ₄	0.73	3.61	<i>J. Phys. Chem. C</i> 2021 , 125, 24805-24813
Co(tpfcBr ₈)/BP2000	0.5 M H ₂ SO ₄	0.75	3.60	<i>Angew. Chem. Int. Ed.</i> 2015 , 54, 14080-14084
CNT-Co-TPFC	0.5 M H ₂ SO ₄	0.62	3.60	<i>Electrochim. Acta</i> 2015 , 171, 81-88
CNT-CoP	0.5 M H ₂ SO ₄	0.65	3.93	<i>J. Am. Chem. Soc.</i> 2014 , 136, 6348-6354
CN-CoPor/C	0.1 M HClO ₄	0.47	3.50	<i>J Electroanal Chem.</i> 2022 , 919, 116536
FeTMPPCl-XC72	0.1 M HClO ₄	0.34	3.80	<i>ACS Catal.</i> 2022 , 12, 1139-1149
C-COP-P-Co	0.5 M H ₂ SO ₄	0.56	3.61	<i>Angew. Chem. Int. Ed.</i> 2014 , 53, 2433-2437
CNT-Co-P	0.5 M H ₂ SO ₄	0.51	3.77	<i>Chem. Mater.</i> 2009 , 21, 3234-3241
PloyCoTAC/BP2000	0.5 M H ₂ SO ₄	0.64	3.13	<i>ACS Catal.</i> 2018 , 8, 5024-5031

^aThe potential measured at the half-wave position for electrocatalytic ORR LSVs.

Table S2. Electrocatalytic ORR performance comparison for molecular electrocatalysts under neutral conditions.

Catalyst	Condition	$E_{1/2}$ (V vs RHE) ^a	n	Reference
1-CNT	0.1 M PBS (pH 7)	0.70	3.88	This work
2-CNT	0.1 M PBS (pH 7)	0.66	3.70	This work
3-CNT	0.1 M PBS (pH 7)	0.67	3.61	This work
Co-cor/Fe ₃ O ₄ NR/TM	0.1 M PBS (pH 7)	0.39	3.75	<i>Angew. Chem. Int. Ed.</i> 2019 , <i>58</i> , 18883-18887
Cu-CTF/CP	0.1 M PBS (pH 7)	0.39	3.75	<i>Angew. Chem. Int. Ed.</i> 2015 , <i>54</i> , 11068-11072
Cu-MWCNTs	0.1 M PBS (pH 7)	0.44	3.30	<i>Angew. Chem. Int. Ed.</i> 2016 , <i>55</i> , 2517-2520
CNT-Co-TPFC	0.1 M PBS (pH 7)	0.38	3.70	<i>J. Phys. Chem. C</i> 2021 , <i>125</i> , 24805-24813
FeTPPS/CuTerpyCD ₂	0.1 M PBS (pH 7)	0.21	3.30	<i>Chem. Sci.</i> 2018 , <i>9</i> , 1989-1995
TPPS-Co/PPY-Au	0.1 M PBS (pH 7)	0.36	3.84	<i>J. Phys. Chem. C</i> 2007 , <i>111</i> , 11216-11222
Fe ₃ O ₄ @N/Co-C	0.1 M PBS (pH 7)	0.55	3.60	<i>J. Mater. Chem. A</i> 2016 , <i>4</i> , 9303-9310
RGO/ZnPc	0.1 M PBS (pH 7)	0.25	3.82	<i>Microsc. Microanal.</i> 2019 , <i>25</i> , 1416-1421
CNT-FePc	0.1 M PBS (pH 7)	0.65	3.85	<i>Electrochim. Acta</i> 2016 , <i>190</i> , 388-395
CoPc/CDC	0.1 M PBS (pH 7)	0.40	3.50	<i>Sustain. Energy Fuels</i> 2019 , <i>3</i> , 3525-3537
Co-PB-1	0.1 M PBS (pH 7)	0.63	2.10	<i>Angew. Chem. Int. Ed.</i> 2020 , <i>59</i> , 4902-4907

^aThe potential measured at the half-wave position for electrocatalytic ORR LSVs.